

Z. LIPNICKI*, K. PANTOL**, B. WEIGAND***

ROLE OF THE CONTACT LAYER IN CONTINUOUS CASTING OF THIN METAL RODS

WPŁYW WARSTWY KONTAKTU NA PROCES ODLEWANIA CIĄGŁEGO CIENKICH PRĘTÓW METALOWYCH

An analytical heat transfer model has been development and applied for calculating the shape of the solid thickness profile for continuous casting of thin metal rods. The stationary solidification front relative to the crystallizer was received from superposition of the motions of the liquid metal flow in the axial direction and the solidifying metal in the radial direction. The shape of the solidified crust depends on several parameters. The influence of the contact layer between the frozen crust and the internal surface of a crystallizer on the solidification process is also studied. The results are presented as an analytical model and are graphically shown for different selected parameters.

Keywords: continuous casting, solidification stationary front, contact layer

W pracy bada się analitycznie i oblicza się kształty frontów krzepnięcia przy odlewaniu ciągłym cienkich metalowych prętów. Określono stacjonarny front krzepnięcia względem krystalizatora przez superpozycję dwóch ruchów: przepływu ciekłego metalu w kierunku pionowym i rozprzestrzenianie się frontu krzepnięcia w kierunku promieniowym. Szczególną uwagę zwrócono na opór cieplny warstwy kontaktu między metalem i powierzchnią wewnętrzną krystalizatora. Wykazano zależność kształtu frontu krzepnięcia od parametrów termodynamicznych i przepływowych metalu. Wyniki badań wybranych metali przedstawiono w formie graficznej.

Nomenclature

λ	–	thermal conductivity, $[W/(m \cdot K)]$
c	–	specific heat, $[J/(kg \cdot K)]$
ρ	–	density, $[kg/m^3]$
L	–	latent heat, $[J/kg]$
u	–	mean velocity of the liquid metal flow, $[m/s]$
H	–	length of crystallizer, $[m]$
R	–	radius of crystallizer, $[m]$
T_F	–	liquid metal fusing point, $[K]$
T_0	–	temperature of cooling water, $[K]$
α_0	–	heat transfer coefficient between channel wall and cooling water, $[W/(m^2 \cdot K)]$
α	–	heat transfer coefficient between liquid metal and crust, $[W/(m^2 \cdot K)]$
α_{CON}	–	heat transfer coefficient in the contact layer, $[W/(m^2 \cdot K)]$
T_W	–	surface temperature, $[K]$
t	–	time, $[s]$
x	–	coordinate, $[m]$
r	–	local values of the solidification front, $[m]$

* INSTITUTE OF ENVIRONMENTAL ENGINEERING, UNIVERSITY OF ZIELONA GÓRA, 65-516 ZIELONA GÓRA, POLAND

** THE STATE HIGHER VOCATION SCHOOL IN GŁOGÓW, 67-200 GŁOGÓW, POLAND

*** INSTITUT FÜR THERMODYNAMIK DER LUFT- UND RAUMFAHRT, UNIVERSITÄT STUTTGART, PFAFFENWALDRING 31, 70569 STUTTGART, GERMANY

The result of the solidification process, the solidified material, is given by the difference between the interface and the center of the channel. Liquid-solid phase-change heat transfer phenomena (solidification) are accompanied by the release of thermal energy. The heat flux per area q released in the interface is transferred through the frozen layer to the crystallizer. We make the simplifying assumption that the solidification front is sharp. We assume that the change of the accumulated heat of the frozen layer is very small. All thermodynamic parameters are assumed to be constant.

2.1. Model-1: Frozen layer with non-perfect conduction ($T_F > \bar{T}$)

The energy balance with equates the latent heat and the heat from the liquid metal flow by convection to the frozen layer can be described as

$$2\pi r\alpha(T_L - T_F) - 2\pi\rho Lr \frac{dr}{dt} = 2\pi\lambda \frac{T_F - \bar{T}}{\ln\left(\frac{r}{R}\right)} = 2\pi R\alpha_{CON}(\bar{T} - T_W) = 2\pi R\alpha_0(T_W - T_0) \quad (2)$$

The expression on the left side of equation (2) contains the heat from the liquid metal flow and the heat flux from the solidified metal. The subsequent expressions show the heat flux through the contact layer and the heat flux transferred to the cooling water.

For the outer surface of the contact layer one obtains from equation (2)

$$T_W = \frac{\alpha_{CON}}{\alpha_{CON} + \alpha_0} \bar{T} + \frac{\alpha_0}{\alpha_{CON} + \alpha_0} T_0 \quad \text{and} \quad (3)$$

$$\bar{T} = \frac{1}{1 + R \frac{\alpha_{CON}\alpha_0}{\alpha_{CON} + \alpha_0} \frac{\ln(R/r)}{\lambda}} T_F + \frac{1}{1 + \frac{\lambda}{\ln(R/r)} \frac{\alpha_{CON} + \alpha_0}{R\alpha_{CON}\alpha_0}} T_0 \quad (4)$$

We now introduce the following non dimensionless variables

$$Ste = \frac{c(T_F - T_0)}{L}; \quad \tau = SteFo; \quad Fo = \frac{at}{R^2}; \quad \tilde{r} = \frac{r}{R}; \quad \frac{1}{Bi_0} = \frac{\lambda}{\alpha_0 R}; \quad \frac{1}{Bi_{CON}} = \frac{\lambda}{\alpha_{CON} R}; \quad \vartheta = \frac{\Delta T}{T_F - T_0} \frac{\alpha R}{\lambda} \quad (5)$$

which are the Stephan number Ste , a dimensionless time τ , a dimensionless radius \tilde{r} , the dimensionless thermal resistance for heat transfer to the coolant Bi_o , the dimensionless thermal resistance of the contact layer, Bi_{CON} and the parameter overheating ϑ .

After substituting the temperature T_w and \bar{T} given by equation (3) and (4) into equation (2) the following equation is obtained for the time depending radius r , describing the solid/liquid interface position from equation (2)

$$\vartheta \tilde{r} - \tilde{r} \frac{d\tilde{r}}{d\tau} = \frac{1}{\beta - \ln \tilde{r}}, \quad (6)$$

where

$$\beta = \frac{1}{Bi_{CON}} + \frac{1}{Bi_0}$$

This equation can be integrated after separating of variables in order to give the solidification time

$$\tau = \int_1^{\tilde{r}} \frac{\tilde{r}(\beta - \ln \tilde{r})}{\vartheta \tilde{r}(\beta - \ln \tilde{r}) - 1} d\tilde{r}, \quad (7)$$

the above equation fulfills the initial condition $\tau = 0, \tilde{r} = 1$.

The solidification time depends on the position of the liquid metal flow relative to the inlet of the crystallizer (see Figures 2, 3). At the inlet of the crystallizer ($x = 0$), the solidification time is equal to zero ($t = 0$) and increases with the distance x according to equation (1). However, the solidification front is stationary relative to the crystallizer, because this situation results from the superposition of both motions: Liquid metal flow in the axial direction x with the mean velocity u and the solidifying metal in the radial direction. The solidification time is defined by equation (1).

The above analysis shows that the stationary interface can be expressed by the following equation. From equations (1) and (7) it follows

$$\tilde{x} = \frac{Re Pr \tilde{a}}{Ste} \int_1^{\tilde{r}} \frac{\tilde{r}(\beta - \ln \tilde{r})}{\vartheta \tilde{r}(\beta - \ln \tilde{r}) - 1} d\tilde{r} \quad (8)$$

In this equation, the dimensionless quantities are defined accordingly to

$$\tilde{x} = \frac{x}{R}, \quad Re = \frac{uR}{\nu}, \quad Pr = \frac{\nu}{a_L}, \quad \tilde{a} = \frac{a_L}{a}. \quad (9)$$

If the liquid metal is not overheated, $\vartheta = 0$, equation (6) reduces to

$$-\tilde{r}(\beta - \ln \tilde{r}) \frac{d\tilde{r}}{d\tau} = 1. \quad (10)$$

The solution of the above equation with the initial condition $\tau = 0, \tilde{r} = 1$ can be obtained easy

$$\tau = \frac{\tilde{r}^2}{2} \ln \tilde{r} + \frac{2\beta + 1}{4} (1 - \tilde{r}^2) \quad \text{and} \quad (11)$$

$$\tilde{x} = \frac{Re Pr \tilde{a}}{Ste} \left[\frac{\tilde{r}^2}{2} \ln \tilde{r} + \frac{2\beta + 1}{4} (1 - \tilde{r}^2) \right]$$

2.2. Model-2: Frozen layer with perfect conduction ($T_F = \bar{T}$)

Assuming the frozen layer with perfect conduction, so that $\bar{T} = T_F$, equation (2) can be simplified to give

$$2\pi r\alpha(T_L - T_F) - 2\pi\rho Lr \frac{dr}{dt} = 2\pi R\alpha_{CON} \cdot (T_F - T_W) = 2\pi R\alpha_0(T_W - T_0) \quad (12)$$

For the outer surface of the contact layer one obtains from equation (12)

$$T_W = \frac{\alpha_{CON}}{\alpha_{CON} + \alpha_0} T_F + \frac{\alpha_0}{\alpha_{CON} + \alpha_0} T_0. \quad (13)$$

After substituting the temperature T_w , given by equation (13), into equation (12) the following equation is obtained for the time depending radius r , describing the solid/liquid interface position

$$r\alpha(T_L - T_F) - \rho Lr \frac{dr}{dt} = R \frac{\alpha_0 \alpha_{CON}}{\alpha_0 + \alpha_{CON}} (T_F - T_0). \quad (14)$$

Introducing the dimensionless variables from equation (6), equation (14) can be written as follows

$$\beta \vartheta \tilde{r} - \beta \tilde{r} \frac{d\tilde{r}}{d\tau} = 1. \quad (15)$$

By using the initial condition that for $\tau = 0, \tilde{r} = 1$, the solidification time and the position of the solidified crust can be obtained as

$$\tau = \frac{1}{\vartheta^2 \beta} \left[\ln \frac{1 - \beta \vartheta \tilde{r}}{1 - \beta \vartheta} - \beta \vartheta (1 - \tilde{r}) \right] \text{ and} \quad (16)$$

$$\tilde{x} = \frac{Re Pr \tilde{a}}{Ste} \frac{1}{\vartheta^2 \beta} \left\{ \ln \left[\frac{1 - \beta \vartheta \tilde{r}}{1 - \beta \vartheta} \right] - \beta \vartheta (1 - \tilde{r}) \right\}.$$

In this equation, the dimensionless quantities are defined accordingly to (5) and (9). As is can be seen by using the rule of L'Hospital equations (16) reduces to equations (17) in the limit when ϑ tends to zero

$$\tau = \frac{1}{2\beta} (1 - \tilde{r}^2) \text{ and } \tilde{x} = \frac{Re Pr \tilde{a}}{2Ste} \beta (1 - \tilde{r}^2). \quad (17)$$

3. Results and discussion

The shapes of the solidified crusts for different external conditions are given in Figures 3, 4, 5. In order to show the quantitative impact of the thermodynamic parameters on the solidification process the corresponding graphs are prepared.

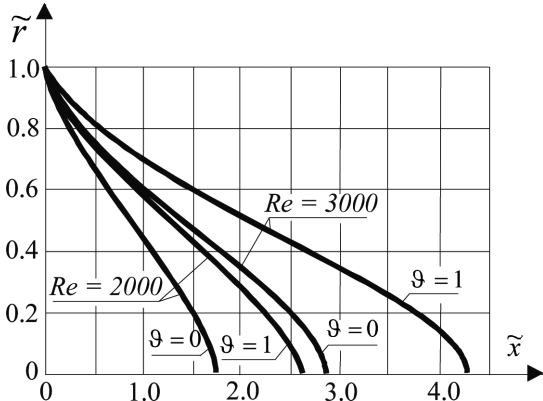


Fig. 3. Solidification front for the liquid metals for $Pr = 0.01$, $Ste = 4$, $\beta = 0.2$, $\tilde{a} = 1.0$

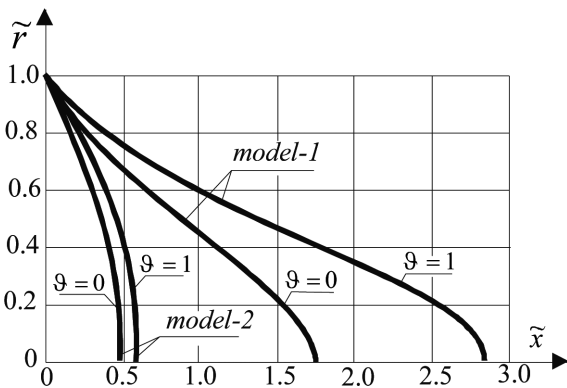


Fig. 4. Comparison of the two solidification models for $Pr = 0.01$, $\beta = 0.2$, $Re = 2000$, $Ste = 4$, $\tilde{a} = 1.0$

Figures 3-5 show shapes of the solidification front for different Reynolds numbers and given values of Pr , Ste and different overheat parameters ϑ and different Biot numbers β . As it can easily be seen, the shape and size of the solidification front depend on the resistance of the contact layer $\lambda/(\alpha_{CON}R)$, the parameter ϑ , the Prandtl number Pr and the Reynolds number Re . From the obtained solution it can be seen that the size of the solidification front grows for increasing values of the Reynolds number, the Prandtl number, the resistance of the contact layer and the parameter ϑ .

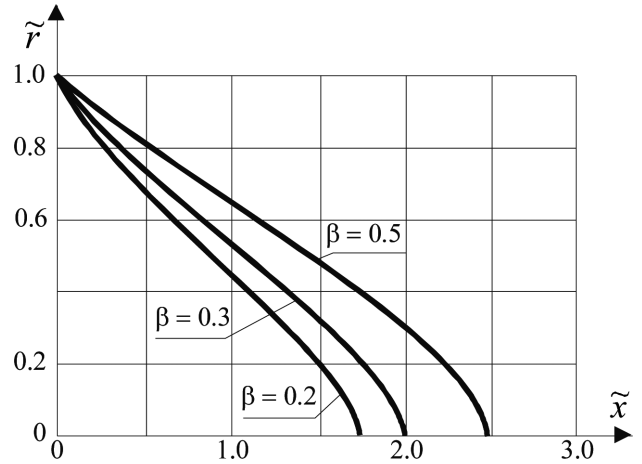


Fig. 5. Solidification front for different values of the parameter β for not overheated liquid metals ($Pr = 0.01$, $Re = 2000$, $Ste = 4$, $\tilde{a} = 1.0$)

Figure 4 shows that there is a substantial difference between the results of model-1 and model-2. The simplification of neglecting the resistance of the frozen layer is thus not justified and will lead to wrong physical results.

Figure 5 shows that the role of the contact layer between the metal and the surface of the cooling channel (parameter β) is very important and might dominate in the continuous casting of a thin metal rod.

As can be seen the maximum length of the liquid metal flow corresponds to the radius $\tilde{r} = 0$ and is equal to

$$\tilde{x}_{\max} = \frac{Re Pr \tilde{a}}{Ste} \int_1^0 \frac{\tilde{r}(\beta - \ln \tilde{r})}{\vartheta \tilde{r}(\beta - \ln \tilde{r}) - 1} d\tilde{r}. \quad (18)$$

The elevation of the interface should not exceed the height of the mold. This may result in an interruption of the continuous casting process. In addition, the maximum length should satisfy the additional condition

$$\tilde{x}_{\max} R \rho g < p_b, \quad (19)$$

which represents the supply of liquid metal to the mold and guarantees the continuity of the stream.

TABLE 1

Different properties of the metals under investigation. The values are taken from literature [17-20]

metal	T_F K	L kJ/kg	λ W/(m·K)		ρ kg/m ³		a m ² /s ·10 ⁻⁵		ν m ² /s ·10 ⁻⁶		Pr
			liquid	solid	liquid	solid	liquid	solid	liquid	liquid	
copper	1356	204	250	330	8300	8920	5.54	8.81	0.476	0.0086	
aluminium	933	390	104	240	2380	2700	3.39	8.89	0.483	0.0142	
tin	506	59	33	66.8	6978	7298	2.01	4.13	0.267	0.0120	
silver	1233	111	357	382	9320	10490	12.4	15.8	0.425	0.0034	

Table 1 gives the thermodynamic properties of the four metals: copper – Cu, aluminium – Al, silver – Ag and tin – Sn. The values are taken from different references in literature [17-20].

Figures 6-7 show shapes of the solidification fronts of the liquid metals for similar external conditions, that are, both at the same flow rates of the liquid metal and the same cooling conditions for comparison. It can be seen that the liquid silver and the liquid copper solidify fastest.

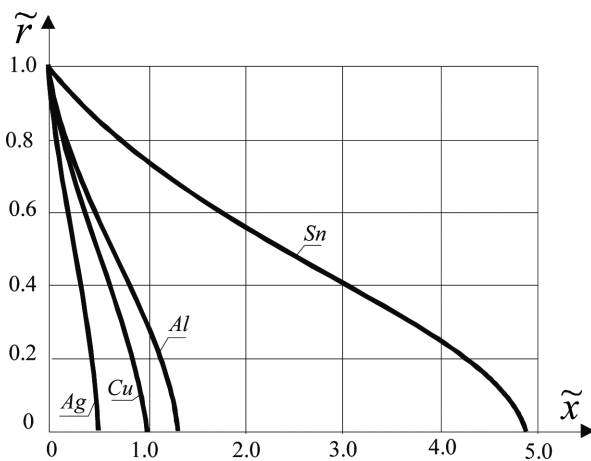


Fig. 6. Solidification front for not overheated liquid metals for $u = 0.05\text{ m/s}$, $R = 0.01\text{ m}$, $\beta = 0.2$, $T_0 = 293\text{ K}$

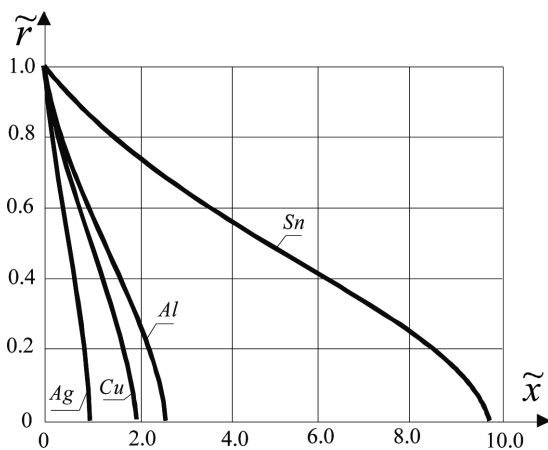


Fig. 7. Solidification front for not overheated liquid metals for $u = 0.1\text{ m/s}$, $R = 0.01\text{ m}$, $\beta = 0.2$, $T_0 = 293\text{ K}$

Aluminium and tin are freezing slowly, so the solidification fronts are more elongated. Knowledge of the shape of

the solidification front, especially the maximum height of the solidification front x_{max} , is needed for determining the technological parameters of the continuous process. The special attention should be paid on the property of metals because of differences given in the literature.

4. Conclusions

The paper focuses on the process of continuous casting of a thin metal rod. The solidification of pure liquid metal in an internal crystallizer flow is investigated and a simplified analytical model is presented. The role of the contact layer between the metal and the surface of the cooling channel is very important and might dominate in the continuous casting of a thin metal rod. A simple analytical model is used to predict the freezing fronts for different metal flows. It is seen that these fronts might differ drastically, depending on the type of metal used. Also the influence of the boundary conditions on the development of the frozen crust can nicely be studied by using the simple model presented here.

REFERENCES

- [1] R. Grzymkowski, B. Mochnicki, Analiza krzepnięcia wlewka w procesie ciągłego odlewania stali, Krzepnięcie metali i stopów **2**, 69-125 (1980).
- [2] B. Mochnicki, Application of the BEM for numerical modeling of continuous casting, Computational Mechanics **18**, Springer-Verlag, 62-71 (1996).
- [3] A.K. Tieu, I.S. Kim, Simulation of the continuous casting process by mathematical model, Int. J. Mech. Sci. **39**, 2, 185-192 (1997).
- [4] E. Majchrzak, B. Mochnicki, M. Dziewoński, M. Jasiński, Identification of boundary heat flux on the continuous casting surface, Archives of Foundry Engineering **8**, 105-110 (2008).
- [5] T. Telejko, Z. Malinowski, M. Rywotyci, Analysis of heat transfer and fluid flow in continuous steel casting, Archives of Metallurgy and Materials **54**, 837-844 (2009).
- [6] L. Sowa, A. Bokota, Numerical model of thermal and flow phenomena the process growing of the CC slab, Archives of metallurgy and materials **56**, 359-366 (2011).
- [7] M. Rywotyci, K. Miłkowska-Piszczyk, L. Trebacz, Identification of the boundary conditions in the continuous casting of steel, Archives of Metallurgy and Materials **57**, 385-393 (2012).

- [8] J.S. Walker, E. Georgopoulos, Slow solidification of a cylinder with constant heat efflux, *Int. Comm. Heat Mass Transfer* **11**, 45-53 (1984).
- [9] T. Loulou, E.A. Artyukhin, J.P. Bardon, Solidification of molten tin drop on a nickel substrate, *10th Int. Heat Transfer Conference*, Brighton, UK **4**, 73-78 (1998).
- [10] T. Loulou, J.P. Artyukhin, J.P. Bardon, Estimation of thermal contact resistance during the first stages of metal solidification process: I – experiment principle and modelisation, *Int. J. Heat and Mass Transfer* **42**, 2119-2127 (1999).
- [11] T. Loulou, J.P. Artyukhin, J.P. Bardon, Estimation of thermal contact resistance during the first stages of metal solidification process: II – experimental setup and results, *Int. J. Heat and Mass Transfer* **42**, 2129-2142 (1999).
- [12] Z. Lipnicki, Role of the contact layer between liquid and solid on solidification process, *Int. J. Heat and Mass Transfer* **46**, 2149-2154 (2003).
- [13] Z. Lipnicki, B. Weigand, A. Bydątek, On the effect of a variable thermal contact resistance on the solidification process, *Archives of Metallurgy and Materials* **50**, 1055-1064 (2005).
- [14] Z. Lipnicki, B. Weigand, Influence of thermal boundary layer on the contact layer between a liquid and a cold plate in a solidification process, *Heat and Mass Transfer* **47**, 1629-1635 (2011).
- [15] Z. Lipnicki, B. Weigand, An experimental and theoretical study of solidification in a free-convection flow inside a vertical annular channel, *Int. J. Heat and Mass Transfer* **55**, 655-664 (2012).
- [16] S. Fukusako, M. Yamada, Solidification of pure liquids and mixtures inside ducts and over external bodies. *Applied Mechanics* **47**, 12, 1, 588-621 (1994).
- [17] R.W. Powell, C.Y. Ho, P.E. Liley, *Thermal Conductivity of Selected Materials*, NSRDS-NBS8, Report- National Standard Reference Data Series National Bureau of Standards, Issued November 25 (1966).
- [18] M.V. Peralta-Martinez, W.A. Wakeham, Thermal Conductivity of Liquid Tin and Indium *International Journal of Thermophysics* **22**, 2, 398 (2001).
- [19] A.A. Mahasneh, A.M. Al-Qararah, S.M.A. Al-Qawabah, Solution of Heat Conduction Equation for a Homogenous Solid Silver Sphere using Homotopy Perturbation Theory, *European Journal of Scientific Research ISSN 1450-216X* **42**, 3, 351-358 (2010).
- [20] H. Shibata, K. Okubo, H. Ohta, Y. Waseda, A novel laser flash method for measuring thermal diffusivity of molten metals/ *Journal of Non-Crystalline Solids* **312-314**, 172-176 (2002).

Received: 10 February 2013.